

Electrophoretic deposition on non-conducting substrates: The case of YSZ film on NiO–YSZ composite substrates for solid oxide fuel cell application

Laxmidhar Besra^{a,*}, Charles Compson^b, Meilin Liu^b

^a Colloids & Materials Chemistry Department, Regional Research Laboratory (CSIR), Bhubaneswar 751013, Orissa, India

^b School of Materials Science and Engineering, Georgia Institute of Technology, 771 Ferst Drive, Atlanta, GA 30332-0245, USA

Received 23 February 2007; received in revised form 23 April 2007; accepted 27 April 2007

Available online 5 May 2007

Abstract

This paper reports the results of our investigation on electrophoretic deposition (EPD) of YSZ particles from its suspension in acetylacetone onto a non-conducting NiO–YSZ substrate. In principle, it is not possible to carry out electrophoretic deposition on non-conducting substrates. In this case, the EPD of YSZ particles on a NiO–YSZ substrate was made possible through the use of an adequately porous substrate. The continuous pores in the substrates, when saturated with the solvent, helped in establishing a “conductive path” between the electrode and the particles in suspension. Deposition rate was found to increase with increasing substrate porosity up to a certain value. The higher the applied voltage, the faster the deposition. For a given applied voltage, there exists a threshold porosity value below which EPD becomes practically impossible. An SOFC constructed on bi-layers of NiO–YSZ/YSZ with YSZ layer thickness of 40 μm exhibited an open circuit voltage (OCV) of 0.97 V at 650 °C and peak power density of 263.8 mW cm^{-2} at 850 °C when tested with H_2 as fuel and ambient air as oxidant.

© 2007 Elsevier B.V. All rights reserved.

Keywords: YSZ; Non-conducting substrate; Electrophoretic deposition; Solid oxide fuel cell

1. Introduction

Electrophoretic deposition (EPD) is a colloidal deposition process assisted and controlled by an electric field [1]. It has been used for the processing and fabrication of a wide variety of advanced ceramic materials and coatings because of the high versatility of its use with different materials and their combinations as well as its cost-effectiveness. While the basic phenomena involved in EPD on a conducting substrate are well known, the specific EPD mechanisms of ceramics on non-conducting substrates are yet to be determined. The EPD of ceramics was first studied by Hamaker [2] in 1940, and only in the 1980s did the process receive attention in the field of advanced ceramics. Although electrophoretic deposition has been applied successfully for many applications, the detailed mechanisms that allow a deposit to be formed are still not entirely clear [3]. Different

explanations to describe the mechanisms for depositing particles with some strength and internal cohesion can be found in literature [1,4]. Fukada et al. [5] presented a comprehensive account of mechanism of deposit formation by EPD. It has been suggested by Bouyer and Foissy [6] that EPD is a two-step process. Under the application of an electric field, the charged particles in the suspension first migrate towards the deposition electrode of opposite charge. The migration depends on the bulk properties of the colloidal dispersion (bath conductivity, viscosity, particle concentration, size distribution, and surface charge density) and the actual field strength in the bath. In a second step the charged particles approach each other and coagulate at or near the surface of the deposition electrode forming a solid deposit layer. It has been suggested that the primary function of the applied electric field is to accelerate the charged particles towards the electrode of opposite charge with the electrostatic coulomb force as the driving force. Sarkar and Nicholson [1] inserted a dialysis membrane between the EPD electrode in an Al_2O_3 suspension. The membrane is permeable to ions but a dense deposit formed thereon and current passed via ionic discharge at the cathode.

* Corresponding author. Tel.: +91 6742581635; fax: +91 6742581637.
E-mail address: ldbbsra@yahoo.com (L. Besra).

They concluded that majority of charge is carried by ions which results in passage of current. But, Zhang and Lee [7] found that current drops dramatically when an insulating polymer film is inserted perpendicular to the electric field between the electrodes. This drop was not observed when the film was placed parallel to the electric field. They suggested that the primary carriers of charge in a EPD process are the particles and the blockage of current was a result of particle movement and not because of an increase in the suspension resistance due to the polymer film. The deposition step proceeds by a complex superposition of electrochemical and aggregation phenomena. Some of the suggested mechanisms in the literature are: (i) flocculation by particle accumulation [2], (ii) particle charge neutralization mechanism [8], (iii) electrochemical particle coagulation mechanism [9], and (iv) the electrical double layer distortion and thinning mechanism [1]. Until recently, the electrical double layer distortion and thinning mechanism is most widely accepted for electrophoretic deposition on conducting substrates.

One of the pre-requisite for electrophoretic deposition is that the substrate should be electrically conductive. In fact, most EPD processes reported in the literature are on electrically conductive metallic or carbon/graphite substrates. In some instances, the deposition substrate has been subjected to heat treatments in reducing atmospheres [10] or sputtering of a conducting coating (e.g. platinum) [11] to make it electrically conductive before EPD. If it were possible to deposit on non-conducting substrates, the EPD process would be more attractive for applications in a wide spectrum of materials processing. There are only a few literature [12–15] in which attempts have been made to electrophoretically deposit on non-conducting substrates. Hamagami et al. [12] studied the fabrication of a ceramic membrane filter by EPD onto porous ceramic substrate, but the target of their study was not to obtain dense and gas-tight membrane. Matsuda et al. [13] used a thin layer of graphite coating on one side of the non-conducting NiO–YSZ porous substrate before EPD. The YSZ films were deposited on the other side of the substrate that did not contain the graphite layer. Such preparatory step, however, make the EPD process more expensive. Negishi et al. [14] investigated preparation of thin and dense mixed conducting layer oxide layer of $\text{La}_{0.8}\text{Sr}_{0.2}\text{Co}_{0.8}\text{Sr}_{0.2}\text{O}_{3-\delta}$ (LSCF) on a porous tubular alumina substrate using EPD technique. But the pore size and porosity of the alumina substrate was arbitrarily chosen at $0.52\ \mu\text{m}$ and 32%, respectively. Similarly, Kanamura and Hamagami [15] also used an arbitrarily chosen porous alumina tube as substrate for deposition of fine particle as thin separation layer on it for use as ceramic membrane filter. More systematic investigation is necessary to ascertain the minimum porosity necessary for electrophoretic deposition. Recently, we reported electrophoretic deposition of YSZ films on green deposits of NiO–YSZ composite layer which were previously deposited electrophoretically on thin discs of carbon sheets [16]. The NiO–YSZ deposit along with the carbon sheet substrate was transferred into a YSZ bath followed by constant voltage EPD for the deposition. The deposition of YSZ was possible only when the NiO–YSZ substrate was saturated with solvent. No deposition was possible on completely dried substrates. The carbon sheets gets burnt off during subsequent

sintering stage, leaving behind a porous NiO–YSZ with a thin and dense YSZ layer on it.

In this paper, we present conditions under which electrophoretic deposition of YSZ is made possible on non-conducting NiO–YSZ substrates to eliminate the need for heat treatment in reducing atmospheres or the need for coating a conductive backing electrode. Further, the suitability of the YSZ film thus deposited has been evaluated for solid oxide fuel cell (SOFC) application.

2. Experimental procedure

2.1. Materials

The YSZ powder used for deposition was commercial grade 8 mol% Y_2O_3 stabilized ZrO_2 powder (Tosoh, TZ-8YS) with average particle size of about $0.5\ \mu\text{m}$. Two types of NiO powders were used. The commercial powder (referred to as NiO-comm hereafter) obtained from J.T. Baker contained relatively larger particles (with average particle size $<10\ \mu\text{m}$). It was milled in ethanol medium for 96 h to less than $5\ \mu\text{m}$ size (referred to as NiO-milled hereafter). The other batch of NiO powder (referred to as NiO-GNP hereafter) was synthesized in our laboratory using the glycine-nitrate process (GNP) [17]. The powders were then ball-milled in ethanol for 48 h and dried prior to use. Acetylacetone (Alfa Aesar, USA) was used as the solvent for preparation of YSZ suspensions.

2.2. Substrate preparation

Substrates for deposition of YSZ were prepared by dry pressing 60:40 weight ratio of NiO:YSZ using a uniaxial hydraulic press (Specac, USA), followed by pre-sintering in air at $1000\ ^\circ\text{C}$ for 4h. The NiO used in the 60:40 weight ratio of NiO:YSZ was a 50:50 weight ratio of NiO-milled and NiO-GNP. Substrates of different porosity were prepared by thorough mixing of different amounts of rice starch as binder with NiO and YSZ powders before pressing. The binder gets burnt off during subsequent firing, leaving behind NiO–YSZ pellets of different porosity.

2.3. Suspension preparation

The first step in electrophoretic deposition is to prepare a stable, agglomerate-free and stable suspension of the ceramic particles in a solvent suitable for development of adequate surface charge on the particles in order to enhance deposition rate and produce homogeneous and crack free deposit. Homogeneous and stable suspensions of YSZ were prepared by dispersing known weights of the powders in a solvent by sonicating in a high intensity ultrasonic bath in order to break up agglomerates. It was equilibrated for 24 h and sonicated again before electrophoretic deposition. Among several solvents studied, acetylacetone was found to be the best in terms of stability of the suspension and deposition quality. In contrast to many EPD processes where it needs addition of suitable additives like binders, there was no necessity of any dispersing agent or binder

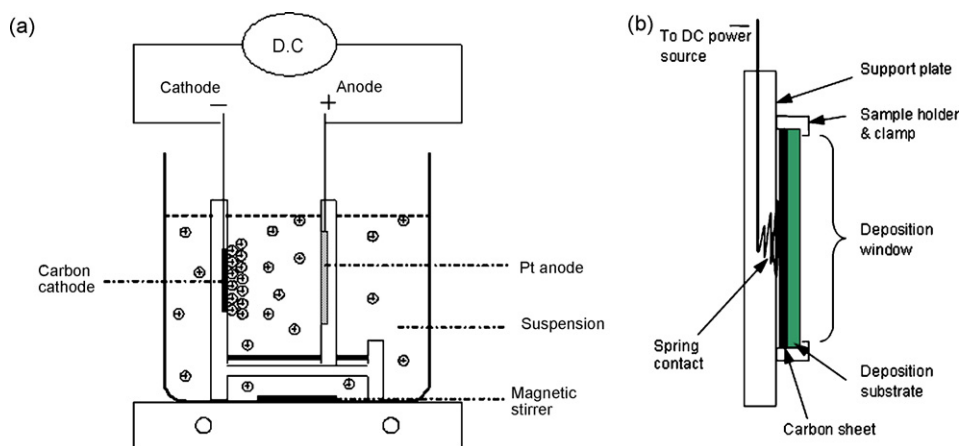


Fig. 1. A schematic diagram of the (a) electrophoretic deposition setup; (b) magnified view of cathode electrode holder showing spring contact and carbon sheet support.

addition when acetylacetonone was used as the solvent. It was adequate for development of positive surface charge on YSZ owing to the presence of some residual water in it which is responsible for charging in a manner similar to that in aqueous medium [18]. The positive charges facilitated migration of the particles towards the oppositely charged cathode during EPD. Therefore, subsequently all the deposition experiments were conducted using acetylacetonone as the solvent. A solid concentration with good suitability for EPD was found to be about 10 g L^{-1} by trial and error approach. Following our previous communication [16] a solid concentration of 10 g L^{-1} was maintained in all the deposition experiments.

2.4. Deposition procedure

The deposition experiments were conducted using a setup used for electrophoretic deposition on flat surfaces as described elsewhere [16]. It consists of two electrode holders made of Teflon, as the principal components and is shown in Fig. 1a. One of the electrode is fixed and the other is movable and can slide along two parallel rods at the bottom so that the distance between the electrodes can be adjusted to a desirable position.

Each of the electrode holders has a circular window facing each other to allow fix the electrodes on it. The deposition electrode (NiO:YSZ) was mounted on the fixed holder and served as the cathode whereas a platinum disc served as the counter-electrode mounted on the movable holder. The deposition electrode was connected to the dc power supply terminal through a spring contact with an intervening carbon sheet in between the substrate and the spring (Fig. 1b). The carbon sheet served two purposes. First it ensured uniform distribution of pressure from the spring onto the substrate and prevented cracking of the sample which happened invariably in absence of this carbon sheet. Although the fuel cell substrate had adequate mechanical integrity, the pressure from the spring on the back side of the substrate was not uniform throughout its area as the size of the spring was relatively smaller than the size of the substrate. Such uneven pressure led to cracking of the substrate. The

cracking problem was eliminated by using an intervening carbon sheet of same area as that of the substrate. It also served as a conductive backing, similar to that used by Matsuda et al. [13], facilitating better deposition. But in the present case, the carbon sheet can be re-used again. Unless otherwise mentioned, a spacing of 15 mm was maintained between the two electrodes in all of our EPD experiments. The holders along with the electrodes were dipped into the reservoir containing the suspension of YSZ. Sedimentation of the particles was prevented by slow stirring by a magnetic bead stirrer as shown in the figure. Electrophoretic deposition experiments were carried out at constant voltages varied in the range from 25 to 100 V, using a high voltage dc power supply unit (Model PS 310) from Stanford Research Systems, USA, with deposition times from 1 to 3 min. The positively charged YSZ particles get deposited on the cathode. The area of the substrate exposed for deposition to occur was maintained constant at 1.0825 cm^2 .

3. Results and discussion

3.1. Characteristics of the substrates

EPD describes the deposition of particles in a suspension onto an electrode under the action of an electric field. Conventionally for electrophoretic deposition, the substrate is needed to be electrically conducting [19,20]. However, we have established, here through this investigation, that EPD can happen even on non-conducting substrates provided it has sufficient porosity to ensure existence of a conductive path through the porous substrate. Haber [21] presented a mathematical analysis of electrophoretic penetration of colloidal ceramic particles into an impermeable porous graphite substrate. Three driving forces for EPD were identified and used to predict penetration depth of single ceramic particle into the porous substrate under the influence of electric potential gradient. The driving forces include (i) the hydrodynamic drag force exerted on the particles due to the electroosmotic flow of the solvent inside the pores, (ii) the electrophoretic force exerted on the particles, and (iii) the stochastic Brownian force due to thermal fluctua-

Table 1
NiO–YSZ substrates of different porosity used for electrophoretic deposition

Sample no.	Starch (%)	Properties of pellet after pre-firing at 1000 °C for 4 h					
		Dry weight (gm)	Diameter (mm)	Thickness (mm)	Volume (mm ³)	Bulk density (g cm ⁻³)	Porosity ^a (%)
P1	10	0.2390	12.82	0.72	92.94	2.5715	60.49
P2	20	0.2363	12.80	0.68	87.50	2.7005	63.85
P3	30	0.2025	12.70	0.77	97.54	2.0761	68.10
P4	40	0.1850	12.38	0.86	103.52	1.7871	72.55
P5	50	0.1712	12.15	0.87	100.87	1.6972	73.93
P6	70	0.1951	12.60	0.95	118.45	1.6471	74.69

^a Theoretical composite density of 60% NiO and 40% YSZ = 6.51 g cm⁻³.

tions of the solvent molecules. Substrates (samples P1–P6) of different porosity were prepared by dry pressing 60:40 weight ratio of NiO and YSZ with different content of rice starch (as given in Table 1) into pellets of 13 mm diameter using uni-axial hydraulic press. The as pressed pellets had good strength, but breaks during clamping onto the EPD electrode holders even with the presence of a carbon sheet. Therefore, the green pellets were pre-fired at 1000 °C for 4 h to impart strength to the pellets. This was associated with some shrinkage of the pellets leading to some loss of porosity. NiO–YSZ substrates of different porosity were obtained by varying the content of rice starch. The properties of the pellets after pre-firing at 1000 °C are given in Table 1. The variation in substrate porosity with starch content is shown in Fig. 2. The porosity have been found to increase almost linearly upto about 40% starch content. Further addition of starch practically does not produce substrates with higher porosity. This is because the shrinkage during pre-sintering at 1000 °C is also higher for substrates with higher starch content.

3.2. Influence of substrate porosity on electrophoretic deposition

In order to isolate the influence of substrate porosity, constant voltage EPD were conducted for a fixed deposition time of 3 min at 25 and 100 V applied potentials. The results are shown

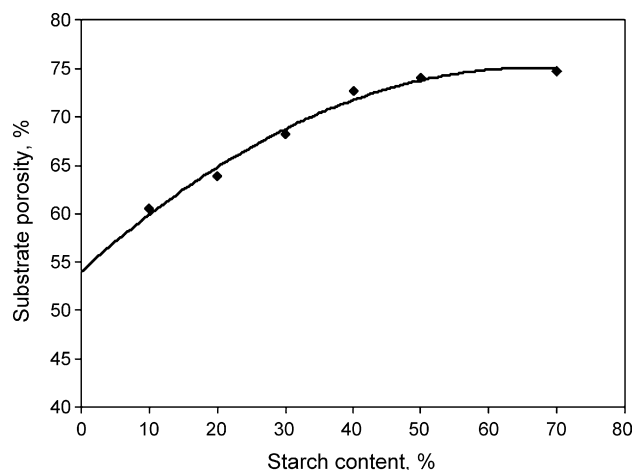


Fig. 2. Variation in NiO–YSZ substrate porosity with starch content after sintering at 1000 °C for 4 h.

in Fig. 3. The deposition of YSZ was found to increase with increasing substrate porosity at both the applied potentials of 100 and 25 V. The deposition rate appears to increase rapidly with porosity and then reach a plateau. In a constant voltage EPD, this is expected because while the potential difference between the two electrodes was kept constant, the formation of insulating layer of deposited ceramic particles on the surface of the deposition electrode will be fast for high porosity substrates in comparison to the low porosity substrates. Thus, the electric field influencing electrophoresis decreases faster for high porosity substrates than for the low porosity ones.

Extrapolation of the deposition curves to the zero deposition value intersects the x-axis at 52.5 and 58.5% porosity for 100 and 25 V applied potentials, respectively. This is significant and serves as the minimum threshold porosity of the substrate for EPD to happen. It has been observed that for a given applied potential, deposition by EPD happens only when the substrate porosity exceeds this value. No deposition is possible if the substrate porosity is below this value. The threshold porosity for 25 V applied potential is higher than the threshold porosity for 100 V applied potential (Fig. 3). The deposit weight increases with increasing substrate porosity. The weight increase is rapid in the region of lower porosity and it tends to reach a plateau after certain porosity value. Also, the deposition is faster for higher applied voltage over the entire range of porosity.

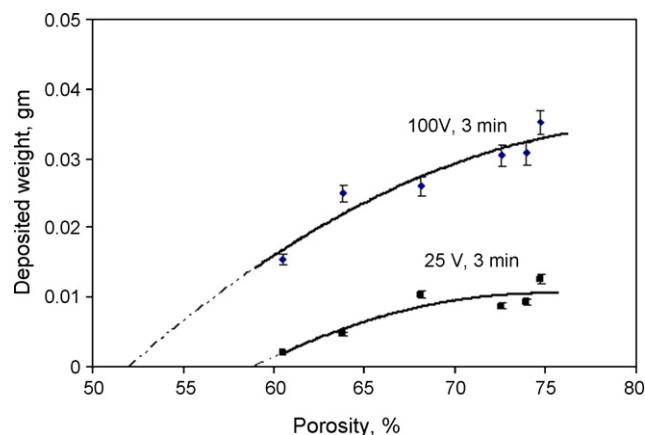


Fig. 3. Influence of substrate porosity on electrophoretic deposition of YSZ on NiO–YSZ cermet from its suspension in acetylacetone [deposition area: 1.0825 cm²].

3.3. Mechanism of deposition

When it comes to electrophoretic deposition on non-conducting substrates, as in the present case, the mechanisms suggested for conducting substrates does not appear to be applicable. The principal concern is how does a non-conducting substrate ensure the existence of uniformly distributed electric field in front of it. The presence of an electrically non-conducting substrate will normally tend to block the conducting path from the electrical contact to the particles in suspension. Since electrophoretic deposition is based on mobility of the particles on application of an electric field, deposition would not happen on a non-conducting substrate. However, the deposition of YSZ on NiO–YSZ substrate in the present case is unique since it makes deposition possible on a non-conducting substrate. We believe that some sort of electrical contact is being developed between the substrate and the particles in the solvent. Two possibilities can be presumed: (i) when a dc potential is applied, the current moves along the surface of the wetted surface rather than through it and (ii) the porous substrates when saturated with the solvent, allows for development of a “conductive path” between the electrical contact and the particles in suspension. However, in another communication [22], we observed that no deposition happened on dense non-conducting NiO–YSZ substrates (obtained by pre-firing at 1400 °C). Therefore, the first possibility is insufficient and can be ruled out. The second assumption of creation of a “conductive path” between the electrical contact and the particles through the pores in the substrate, seem more realistic. This is shown schematically in Fig. 4.

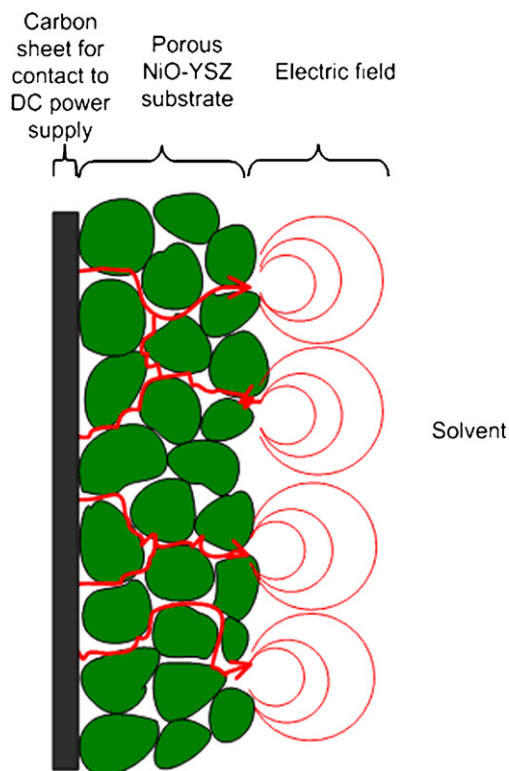


Fig. 4. Conceptual representation of possible EPD mechanism on non-conducting substrates with a conductive backing of carbon sheet.

However, this mechanism of “conductive path” through porous substrate by saturation with solvent may probably be applicable for substrate with interconnected porosity only. Presence of only closed pores in the substrate will tend to block the “conductive path” preventing any electrophoretic deposition. Matsuda et al. [13] also reported deposition of YSZ on NiO–YSZ substrate by EPD, but it can be viewed as deposition on a conductive graphite substrate with increased electrical resistance due to NiO–YSZ layer. For this reason a relatively high deposition voltage of 400–900 V was necessary for EPD. Our method is different from that of Matsuda et al. [13] in that we did not coat but there was a spring contact (with an intervening carbon sheet sandwiched) of the substrate with the dc power supply. The carbon sheet could be re-used again for many depositions. Secondly, good deposition was achieved even at applied voltage of as low as 25 V in the present case. Unlike multiple deposition and sintering steps adopted by other investigators [23,24], our approach enabled obtaining dense and gas-tight films in a single deposition and sintering step as discussed in the next section.

3.4. Characteristics of deposited YSZ film

The deposited YSZ film on NiO–YSZ substrates were sintered at 1400 °C for 4 h. Fig. 5 shows the surface and cross-sectional SEM image of YSZ film on NiO–YSZ substrate of 72.55% porosity (Sample No. P4) deposited at 100 V for 3 min. The surface microstructure reveal a reasonably dense film with distinct YSZ grains. From the surface microstructure there seem to be some pin holes, but the cross-sectional microstructure reveal that the film is dense. The pin-hole like pores on the surface may be isolated and not interconnected. There was also good interfacial adhesion between the YSZ film and the substrate. The thickness of the YSZ film was about 40 μm. The objective of this investigation was to explore the feasibility of electrophoretic deposition on non-conducting substrates, and not much emphasis was given on optimizing film thickness for further application. It will however be interesting to see what is the minimum thickness of dense and gas-tight film that can be deposited by this approach. This will be addressed in our subsequent communications.

3.5. SOFC performance

The suitability of NiO–YSZ/YSZ bi-layer thus obtained was evaluated for solid oxide fuel cell applications. A single cell was constructed on the bi-layer by painting a layer of cathode on the YSZ film followed by sintering at 1250 °C for 2 h. The cathode composed of 50:50 weight ratio of La_{0.8}Sr_{0.2}MnO₃ (LSM) and YSZ. The fuel cell was sealed to an alumina tube using silver pastes as described elsewhere [16]. The seals were cured as the fuel cell was brought to the testing temperature. Hydrogen gas was used as fuel during testing. Air was used as oxidant and was supplied to the cathode by ambient air flow. The cell-tube apparatus was placed in a furnace and brought to the testing temperature with continuous flow of H₂ gas. Platinum wires were attached to each electrode as the output terminal as electrical collector. The fuel cell performance was measured with a

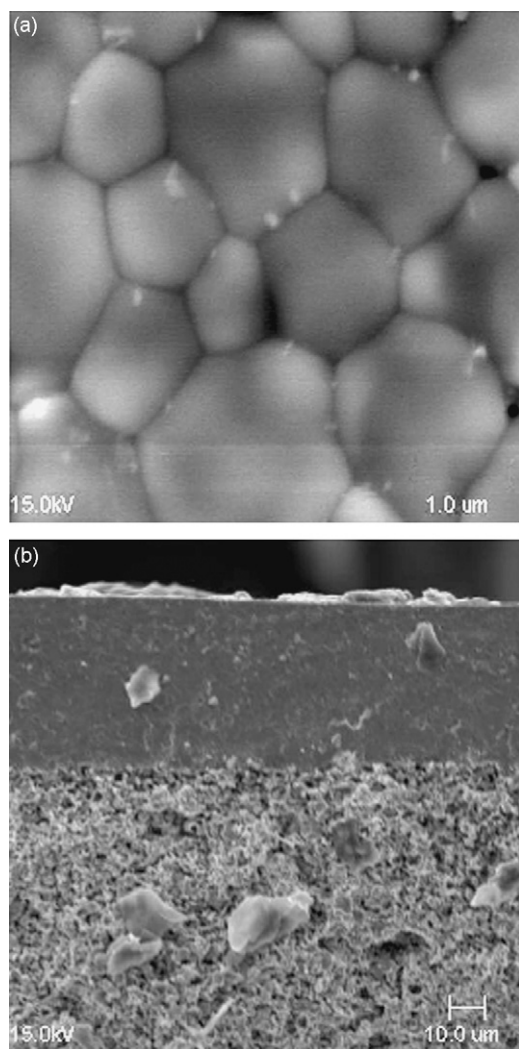


Fig. 5. (a) Surface and (b) cross-sectional SEM image of YSZ film deposited on NiO-YSZ substrate (porosity = 72.55%) at 100 V for 3 min and sintered at 1400 °C for 2 h.

Solartron Potentiostat/Galvanostat (Model SI 1287) interfaced with a computer. The impedances were measured typically in the frequency range from 0.1 to 100 kHz using Solartron 1255 and 1287 interfaced with a computer.

Fig. 6 shows the open circuit voltage (OCV) of the fuel cell constructed on a substrate of 72.55% porosity (sample P4 in Table 1) and tested at different temperatures from 650 through 850 °C. It showed an OCV of 0.97 at 650 °C which dropped to 0.86 at 850 °C. The high OCV value at 650 °C indicate that the YSZ film was reasonably dense. The corresponding power density and impedance exhibited by the fuel cell is shown in Figs. 7 and 8, respectively. Fig. 7 indicate that a peak power density of 263.8 mW cm⁻² was obtained at a corresponding cell voltage of 0.38 V. The total interfacial impedance calculated from Fig. 8 is presented in Table 2. The lower power density value is probably a result of large ohmic drop across the thick YSZ electrolyte (40 μm). Since the objective of this investigation was to explore the feasibility of EPD on non-conducting substrates, we did not conduct optimisation of the conditions for obtaining thin YSZ films. A much higher power density can

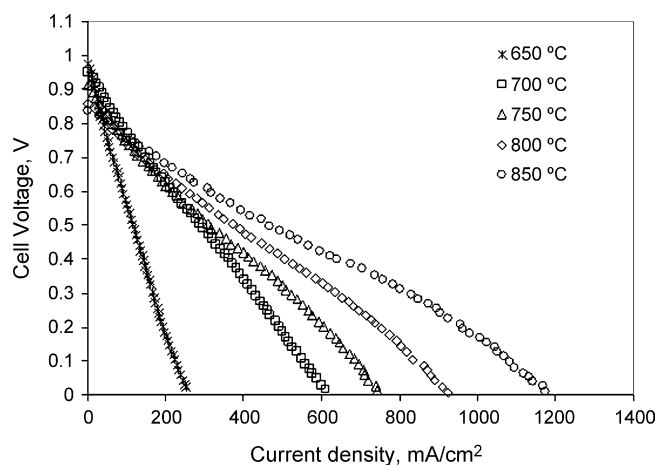


Fig. 6. Cell voltage as a function of operating current density for NiO:YSZ (60:40)/YSZ/LSM:YSZ (50:50) fuel cells constructed on sample P4 [deposition condition of YSZ on NiO-YSZ: 100V, 3 min].

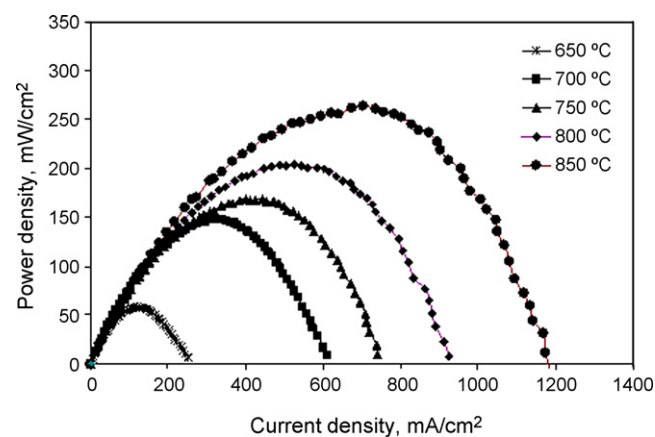


Fig. 7. Power density as a function of operating current density for NiO:YSZ (60:40)/YSZ/LSM:YSZ (50:50) fuel cells constructed on sample P4 [deposition condition of YSZ on NiO-YSZ: 100V, 3 min].

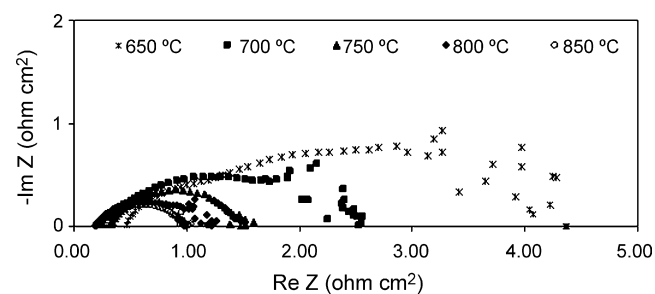


Fig. 8. Impedance spectra of a fuel cell with a configuration of NiO:YSZ (60:40)/YSZ/LSM:YSZ (50:50) under open circuit condition using a two electrode configuration.

Table 2

Total interfacial impedance of the SOFC NiO:YSZ (60:40)/YSZ/LSM:YSZ (50:50) at different operating temperature

Temperature (°C)	Total interfacial resistance (Ω cm ²)
650	3.89
700	2.32
750	1.15
800	1.00
850	0.79

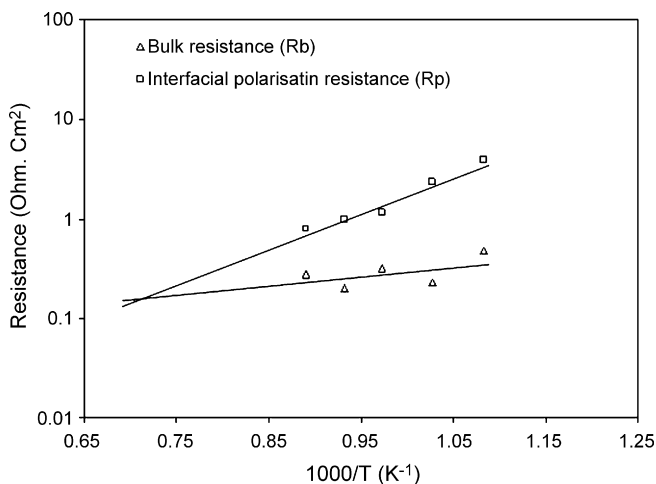


Fig. 9. Interfacial polarization resistance and bulk resistance determined from the impedance spectra presented in Fig. 8.

be expected for thinner ($10\ \mu\text{m}$ or less) electrolyte films. However, the EPD of YSZ on non-conducting NiO–YSZ substrates has been proved and the bi-layer thus obtained has been found to be suitable for fabricating a functional SOFC. Optimising conditions for obtaining thin films to maximise power density of SOFCs will be reported in our subsequent communications. Shown in Fig. 9 are the bulk resistance (R_b) of YSZ film and the interfacial polarization resistances (R_p) as determined from impedance spectroscopy presented in Fig. 8. The total interfacial polarization resistance, which corresponds to the sum of all the resistances arising from electrochemical processes occurring at both electrolyte–electrode interface, decreases from $3.89\ \Omega\ \text{cm}^2$ at $650\ ^\circ\text{C}$ to $0.79\ \Omega\ \text{cm}^2$ at $850\ ^\circ\text{C}$. These values are comparable to the interfacial polarization resistance reported in the literature [25].

4. Conclusions

A method for performing electrophoretic deposition on non-conducting substrates has been developed through the use of substrates of adequate porosity. Good deposition was achieved when the substrate porosity was above a certain threshold value. No deposition was possible when the substrate porosity is below the threshold porosity. The threshold porosity has been found to be lower for a higher applied voltage. The suitability of YSZ film deposited on a non-conducting NiO–YSZ porous substrate was evaluated for SOFC applications. A single cell with configuration NiO–YSZ/YSZ/LSM–YSZ in which the YSZ film was

$40\ \mu\text{m}$ exhibited an open circuit voltage of $0.97\ \text{V}$ at $650\ ^\circ\text{C}$ and a power density of $263.8\ \text{mW}\ \text{cm}^{-2}$ at $850\ ^\circ\text{C}$ when tested with H_2 as fuel and ambient air as the oxidant.

Acknowledgements

A portion of this work was supported by the US Department of Energy SECA Core Technology Program (under Award Number DE-FC26-02NT41572). One of the authors (LB) is thankful to the Department of Science and Technology (DST), Govt. of India, for the BOYSCAST fellowship, and to the Director, Regional Research Laboratory Bhubaneswar, for permission to publish this paper.

References

- [1] P. Sarkar, P.S. Nicholson, *J. Am. Ceram. Soc.* 79 (8) (1996) 1987–2002.
- [2] H.C. Hamaker, *Trans. Faraday Soc.* 36 (1940) 279–283.
- [3] O.O. Van der Biest, L.J. Vandeperre, *Annu. Rev. Mater. Sci.* 29 (1999) 327–352.
- [4] D.R. Brown, F.W. Salt, *J. Appl. Chem.* 15 (1965) 40–48.
- [5] Y. Fukada, N. Nagarajan, W. Mekky, Y. Bao, H.S. Kim, P.S. Nicholson, *J. Mater. Sci.* 39 (2004) 787–801.
- [6] F. Bouyer, A. Foissy, *J. Am. Ceram. Soc.* 82 (8) (1999) 2001–2010.
- [7] J. Zhang, B.I. Lee, *J. Am. Ceram. Soc.* 83 (10) (2000) 2417–2422.
- [8] F. Grillon, D. Fayeulle, M. Jeandin, *J. Mater. Sci. Lett.* 11 (1992) 272–275.
- [9] H. Koelmans, *Phillips Res. Rep.* 10 (1995) 161–193.
- [10] J. Will, M.K.M. Hruschka, L. Gubler, L.J. Gauckler, *J. Am. Ceram. Soc.* 84 (2) (2002) 328–332.
- [11] J. Van Tassel, C.A. Randall, *J. Mater. Sci.* 39 (2004) 867–879.
- [12] J. Hamagami, K. Kanamura, T. Umegaki, *Electrochem. Soc. Proc.* 21 (2002) 55–61.
- [13] M. Matsuda, T. Hosomi, K. Murata, T. Fukui, M. Miyake, *Electrochem. Solid State Lett.* 8 (1) (2005) A8–A11.
- [14] H. Negishi, N. Oshima, K. Haraya, K. Sakaka, T. Ikegami, Y. Idemoto, N. Koura, H. Yanagishita, *J. Ceram. Soc. Jpn.* 114 (1) (2006) 36–41.
- [15] K. Kanamura, J. Hamagami, *Solid State Ionics* 172 (2002) 303–308.
- [16] L. Besra, S. Zha, M. Liu, *J. Power Sources* 160 (2006) 207–214.
- [17] S. Zha, W. Rauch, M. Liu, *Solid State Ionics* 166 (2004) 241–250.
- [18] L. Vandeperre, C. Zhao, O. Van der Biest, in: J. Binner (Ed.), *Proceedings of the Novel Chemistry/Processing Session of the Sixth conference and Exhibition of the European Ceramic Society, Brighton, UK, 20–24 June, 1999*, IOM Communications Ltd., London, 2000, pp. 69–74.
- [19] M.S.J. Gani, *Ind. Ceram.* 14 (1994) 163–174.
- [20] A.R. Boccaccini, C.B. Ponton, *J. Met.* 47 (10) (1995) 34–37.
- [21] S. Haber, *J. Colloid Interface Sci.* 179 (1996) 380–390.
- [22] L. Besra, C. Compson, M. Liu, *J. Am. Ceram. Soc.* 89 (10) (2006) 3003–3009.
- [23] T. Ishihara, K. Sato, Y. Takita, *J. Am. Ceram. Soc.* 79 (4) (1996) 913–919.
- [24] T. Ishihara, K. Shimose, T. Kudo, H. Nishiguchi, T. Akbay, Y. Takita, *J. Am. Ceram. Soc.* 83 (8) (2000) 1921–1927.
- [25] E.P. Murray, S.A. Barnett, *Solid State Ionics* 143 (2001) 265–273.